A new phase in the $LiRbSO_4$-$LiCsSO_4$ system

2000 J. Phys.: Condens. Matter 12 7559

(http://iopscience.iop.org/0953-8984/12/34/303)

J. Phys.: Condens. Matter **12** (2000) 7559–7568. Printed in the UK PII: S0953-8984(00)12952-2

A new phase in the $LiRbSO_4$–$LiCsSO_4$ system

R J C Lima, J M Sasaki, P T C Freire, A P Ayala†, I Guedes, F E A Melo and J Mendes Filho

Departamento de Física, Universidade Federal do Ceará, CP 6030, Fortaleza (CE) 60455-760, Brazil

E-mail: ayala@fisica.ufc.br

Received 29 March 2000, in final form 3 July 2000

Abstract. In this work we have presented a spectroscopic study carried out to determine the room temperature crystal symmetry of $LiCs_{0.5}Rb_{0.5}SO_4$ crystals. On the basis of x-ray and Raman scattering measurements, we have proposed that $LiCs_{0.5}Rb_{0.5}SO_4$ crystallizes in a monoclinic structure belonging to the C_s point group with four molecules per unit cell, where the SO_4 groups, Rb and Cs ions, are distributed into two non-equivalent $C_1(2)$ site symmetries.

1. Introduction

It is well known that compounds belonging to the family of so-called sulphate crystals $LiASO_4$ (A = Na, K, Rb, or Cs) are examples of materials presenting a large variety of structural phase transitions. These compounds are characterized by a distorted tridymite-type structure, which can be described by a framework consisting of six-membered rings of alternating SO_4 and LiO_4 tetrahedra [1, 2]. The variety of the phase transitions is closely related to the rotation of the SO_4 tetrahedra, accompanied by small cation displacements. The formations of numerous ferroelectric and ferroelastic phases of these compounds, as well as some pressure-induced phase transitions [3–5], are also mainly associated with partial or complete ordering of SO_4 tetrahedra [6].

At room temperature, $LiCsSO_4$ (LCS) presents an orthorhombic structure with space group D_{2h}^{16}. Below its Curie temperature ($T_c = 202$ K), it has a monoclinic structure belonging to space group C_{2h}^5 [7]. The physical mechanism for this transition is the anomalous rotation of SO_4 ions around the z-axis. In contrast to LCS, $LiRbSO_4$ (LRS) does not undergo any structural changes for temperatures below 300 K. However, it undergoes many structural phase modifications in the temperature range from 300 to 477 K [6, 8]. Up to 439 K, it has a C_{2h}^5 monoclinic structure (phase V) and goes to a D_{2h}^{16} orthorhombic structure (phase I), at 477 K, after three more phase transformations, namely:

(i) phase IV ($439 < T < 458$ K) where it exhibits a C_s^2 monoclinic structure;
(ii) phase III ($458 < T < 475$ K) where its structure is also monoclinic but belonging to a space group (C_{2h}^5); and
(iii) phase II ($475 < T < 477$ K) where it presents an incommensurated modulation.

From x-ray measurements it is known that the monoclinic angle is very close to 90°, so the distortion of the orthorhombic lattice is very small [6, 8]. Also, due to the group–subgroup

† Author to whom any correspondence should be addressed. Fax: 55 (85) 288.9903.

0953-8984/00/347559+10$30.00

relation between the D_{2h} and C_{2h} point groups, a continuous series of $LiRb_{1-x}Cs_xSO_4$ solid solutions is supposed to exist. Pietrazko [9] have reported x-ray scattering studies on the $LiRb_{1-x}Cs_xSO_4$ system at room temperature for $x = 0.25$, 0.5 and 0.75. They showed that the C_{2h} monoclinic phase of LRS is stable up to $x = 0.5$, and it changes to the D_{2h}^{16} orthorhombic (LCS) structure for $x = 0.75$. Later, Hasebe and Asahi [10] studied the $LiRb_{1-x}Cs_xSO_4$ system at 300 K for low values of x, and showed that in this limit, the crystal presents basically a C_{2h}^5 monoclinic structure. Further results on the $LiRb_{1-x}Cs_xSO_4$ system were reported by Mel'nikova *et al* [11,12]. They used differential scanning calorimetry and birefringence measurements to determine the concentration–temperature phase diagram of the $LiRb_{1-x}Cs_xSO_4$ system. In spite of the good results shown for $x \simeq 0$ and $x \simeq 1$, no information about the structure of $LiRb_{0.5}Cs_{0.5}SO_4$ (hereafter LRCS) was given.

Besides these papers reporting the experimental results, some theoretical calculations on the stability of the structural phase in the $LiRb_{1-x}Cs_xSO_4$ system have also appeared. In reference [13], Katkanant, using lattice and molecular dynamics simulations, showed that a continuous transformation in the room temperature crystal structure of the $LiRb_{1-x}Cs_xSO_4$ system from C_{2h}^5 (LRS) to D_{2h} (CLS) when x goes from 0 to 1 is expected.

In order to provide further information about the crystal structure of $LiRb_{1-x}Cs_xSO_4$ crystals, in this work we present a spectroscopic study using x-ray and Raman scattering techniques to obtain information about the room temperature crystal structure of the LRCS compound. It was observed that LRCS crystallizes in a monoclinic structure with factor group C_s with four formula units per cell, where the four SO_4 ions are in two non-equivalent $C_1(2)$ local site symmetries, the two Rb and two Cs ions each occupy $C_1(2)$ local site symmetries, while the four Li ions are in two $C_1(2)$ local site symmetries.

2. Experimental procedure

Monocrystals of LRCS were grown from saturated solutions containing equal stoichiometric concentrations of $Li2SO_4$, $CsSO_4$ and $Rb2SO_4$ powders in tridistilled water by slow evaporation at controlled temperature (40 °C) and pH (=9). The crystals obtained are transparent and have good optical quality. The choice of the samples used in the experiments was made by using a polarizing microscope, observing the light through the crystallographic axes. The samples used in the Raman measurements had typical dimensions of $3.5 \times 2.0 \times 2.0$ mm^3. X-ray diffraction patterns were obtained using a Rigaku powder diffraction diffractometer operating with Cu Kα radiation at 40 kV/25 mA. The diffraction patterns were taken in stepping scan mode with 5 s counting for each 0.01° step. Raman spectra of LRCS were recorded in a backscattering geometry using a micro-Raman device. The spectrometer used was a Jobin-Yvon T64000 Raman system equipped with an Olympus BX40 microscope and a N_2-cooled charge-coupled device (CCD). The scattering was excited with the 514.5 nm line of an Ar-ion laser. All measurements were performed using a long-working-distance plano-achromatic objective (20X/0.35, 20.5 mm) to avoid the propagation of oblique phonons. Scattering geometries for the spectra listed in the text and figures follow the usual Porto notation, A(BC)D [14].

3. Results and discussion

3.1. X-ray diffraction

In figures 1(a), 1(b) and 1(c) we show the room temperature powder x-ray diffraction patterns of LCS, LRCS and LRS, respectively. As can be observed, the LRS and LCS patterns are quite similar, while LRCS shows a more complex diffraction pattern. The appearance of additional diffracted peaks indicates that LRCS presents a different structure in comparison with those

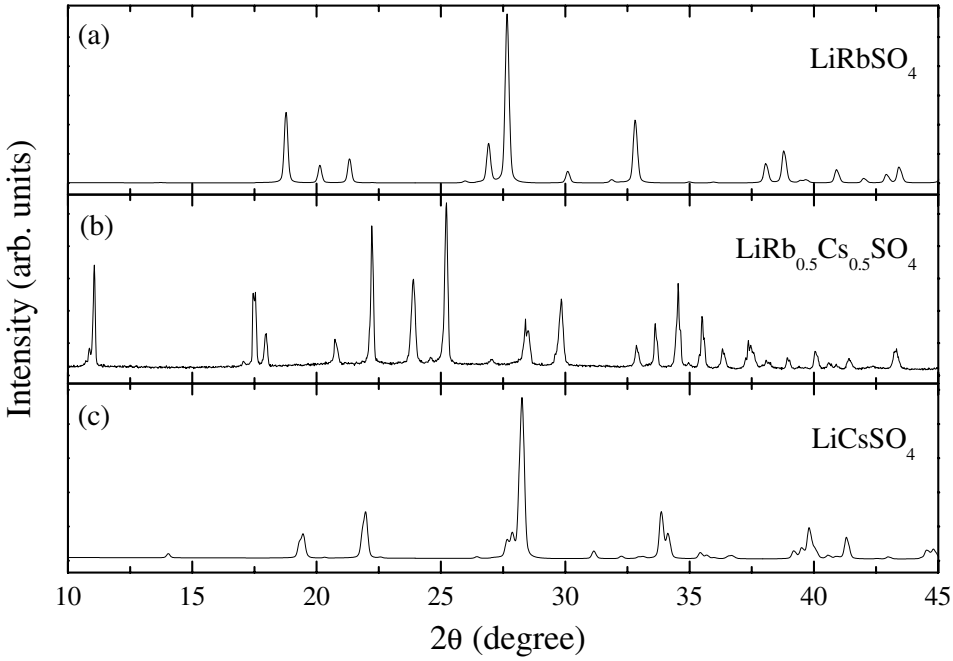

Figure 1. X-ray diffraction patterns of (a) $LiCsSO_4$, (b) $LiCs_{0.5}Rb_{0.5}SO_4$ and (c) $LiRbSO_4$ taken at 300 K.

of LCS and LRS crystals. A rigorous search was made of the ICDD and ICSD databases—powder and single-crystal diffraction databases respectively—and any match was found. The lattice parameters (a, b, c, α, β, γ) were obtained from the powder diffraction pattern using the DICVOL [16, 17] and ITO [18] programs. The results are shown in table 1. While the DICVOL program gave as more probable an orthorhombic symmetry, the result obtained with ITO indicates that the crystal has a small monoclinic distortion. A careful analysis of the powder pattern showed that no extinction rules are operative.

Table 1. Lattice parameters at room temperature obtained by the least-squares method.

	DICVOL91	ITO
a (Å)	15.977(8)	15.983(6)
b (Å)	5.042(3)	5.050(4)
c (Å)	5.184(3)	5.191(7)
α (deg)	90	90
β (deg)	90	90
γ (deg)	90	90.22(7)
Volume (Å^3)	417.64	418.97
FOM	28.6	28.8

From the lattice parameter obtained from these results and the density ρ, we can estimate the number of formula units per unit cell (Z) using the following expression [19]:

$$Z = \rho V/W \times 1.66 \times 10^{-24} \tag{1}$$

where V is the unit-cell volume and W is the formula weight. Using the values presented in table 1, we find $Z = 3.75$, which indicates that LRCS has four formula units per unit cell.

3.2. Raman spectroscopy

In order to complement the result obtained by the x-ray analysis, we have performed Raman measurements using all of the possible scattering geometries, available from backscattering experiments. From the nine possible scattering geometries, we have divided them into four sets of equivalent spectra, namely:

(i) $z(xx)\bar{z}$, $z(yy)\bar{z}$, $z(xy)\bar{z}$;
(ii) $x(yy)\bar{x}$, $x(zz)\bar{x}$;
(iii) $y(xx)\bar{y}$, $y(zz)\bar{y}$; and
(iv) $x(yz)\bar{x}$, $y(zx)\bar{y}$

where x, y and z correspond to the crystalline axes $\boldsymbol{a}$, $\boldsymbol{b}$ and $\boldsymbol{c}$, respectively. In figure 2 we show only one spectrum corresponding to each set in the wavenumber region of the asymmetric stretching mode of the SO_4 group (ν_3). Also, since all spectra are equal each other in the symmetric stretching SO_4 mode (ν_1) wavenumber region, we display only one spectrum as an inset in figure 2(a).

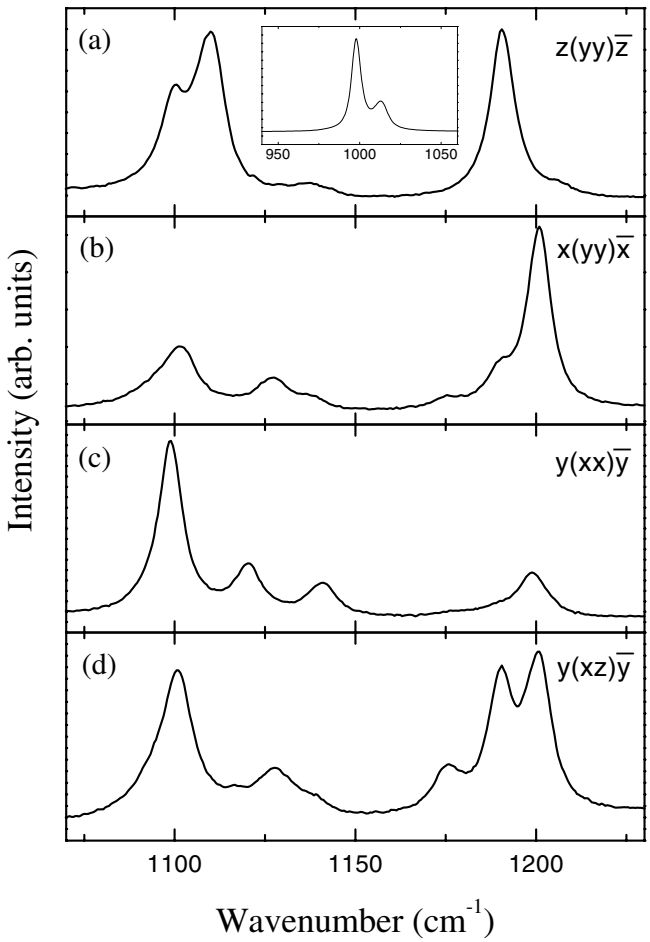

Figure 2. Polarized Raman spectra of LRCS in the wavenumber range of ν_1 (inset) and ν_3 modes at 300 K.

The appearance of two ν_1 modes indicates that the SO_4 ions occupy two non-equivalent site symmetries in the LRCS crystalline structure. As the x-ray diffraction powder pattern analysis suggests that the structure is monoclinic or orthorhombic with four molecules per unit cell, the SO_4 ions should be distributed over two sites with multiplicity two.

The analysis of the ν_3 internal modes allowed us to obtain additional information about the possible space groups. From comparing the $z(yy)\bar{z}$ and $x(yy)\bar{x}$ scattering geometries (figures 2(a) and 2(b), respectively), it is observed that the vibrational bands are shifted depending on the incident light direction, even when the same polarizability tensor (α_{yy}) is excited. This is a characteristic of polar vibrational modes, where the splitting in longitudinal and transverse modes should be observed. As polar modes are only Raman active in crystals without inversion centres, we can infer that LRCS has a non-centrosymmetric structure. Furthermore, the same argument allows us to exclude the D_2 point group because the totally symmetric scattering geometries are non-polar. Thus, the possible point groups for the LRCS crystals are: (i) monoclinic: C_2 or C_s; (ii) orthorhombic: C_{2v}.

In order to choose between these groups, we use the Raman-active modes predicted in each scattering geometry, which we show in table 2. From examining this table and comparing it with the set of equivalent spectra previously described, we can observe that the distribution of the first set is not consistent with the C_{2v} group, since in this group the A_1 modes are active in the $z(xx)\bar{z}$ and the $z(yy)\bar{z}$ scattering geometries, while in the $z(xy)\bar{z}$ geometry the A_2 modes should be observed. Moreover, the selection rules determined by the first and fourth sets are characteristic of monoclinic groups with $\alpha_{xx}, \alpha_{yy}, \alpha_{zz}$ and α_{xy} corresponding to one irreducible representation, while α_{xz} and α_{yz} correspond to another. A similar analysis allows us to exclude C_2, because in this group the second and third sets should be equivalent, while the spectra in the fourth set should not be different. In conclusion, the vibrational mode distributions observed in the measured scattering geometries are only correctly described for the C_s point group.

Table 2. Comparison of the irreducible representations active in the probable point groups

Sets	C_{2v}	C_2	C_s
$z(xx)\bar{z}$			
$z(yy)\bar{z}$	$A_1(LO_z)$	$A(LO_z)$	$A'(TO_x + TO_y)$
$z(xy)\bar{z}$	A_2		
$x(yy)\bar{x}$			
$x(zz)\bar{x}$	$A_1(TO_z)$	$A(TO_z)$	$A'(LO_x + TO_y)$
$y(xx)\bar{y}$			
$y(zz)\bar{y}$			$A'(TO_x + LO_y)$
$x(yz)\bar{x}$	$B_2(TO_y)$	$B(LO_x + TO_y)$	
$y(xz)\bar{y}$	$B_1(TO_x)$	$B(TO_x + LO_y)$	$A''(TO_z)$

From comparing the available sites in the C_s factor groups, we observe that the SO_4 ions can occupy sites with symmetry $C_1(2)$ in the groups C_s^1 or C_s^2, while they would be at $C_s(2)$ sites in C_s^3. We do not consider the C_s^4 space group because it does not have sites with multiplicity two, as required to distribute the SO_4 ions. To decide, among the remaining C_s^1, C_s^2 and C_s^3 space groups, which gives the Raman phonon distribution shown in figure 2, we calculate the internal SO_4-mode distribution in terms of the irreducible representation of the C_s point group by considering that the SO_4 group presents either C_s or C_1 local site symmetries. By using the method of molecular site group analysis described in reference [20], we obtain the distribution shown in table 3.

Table 3. Correlation diagram of the SO_4 ions in C_1 and C_s sites of a C_s point group.

Free-ion symmetry	Site symmetry	Crystal symmetry	Vibrational modes
T_d	C_1	C_1	
$A_1(\nu_1)$	A	A′	$\nu_1, 2\nu_2, 3\nu_3, 3\nu_4$
$E(\nu_2)$			
$F_2(\nu_3, \nu_4)$		A″	$\nu_1, 2\nu_2, 3\nu_3, 3\nu_4$

Free-ion symmetry	Site symmetry	Crystal symmetry	Vibrational modes
T_d	C_1	C_s	
$A_1(\nu_1)$	A	A′	$\nu_1, \nu_2, 2\nu_3, 2\nu_4$
$E(\nu_2)$			
$F_2(\nu_3, \nu_4)$		A″	ν_2, ν_3, ν_4

It should be noted that if SO_4 ions were in C_s local site symmetries, their ν_1 vibrations would be observed only in the A′ symmetry. However, as mentioned above, the ν_1 vibrations are observed in all geometries investigated. In this way, the C_s^3 space group can be ruled out. Unfortunately, from Raman measurements, we cannot decide incontrovertably between C_s^1 or C_s^2 space groups, since they have the same phonon distribution. We can just suppose that due to the fact that no extinction rules were observed to be operative from x-ray measurements, the C_s^1 space group seems to be the most probable.

On the basis of the supposition that LRCS belongs to the C_s point group, the irreducible representations for the external optic vibrational modes can be obtained using the method of site group analysis proposed by Rousseau *et al* [21]. As LRCS has four molecules per unit cell, the two Li, Cs and Rb ions should be distributed in two $C_1(2)$ groups. Table 4 displays how the LRCS translational, rotational and internal modes are distributed in terms of A′ and A″ irreducible representations of the C_s point group.

Table 4. Distribution of LRCS rotational (R), translational (T) and internal (I) modes in terms of the irreducible representations of the C_s factor group.

			Number of vibrations	
Atom		Site symmetry	A′	A″
2Li	T	$C_1(2)$	6	6
Rb	T	$C_1(2)$	3	3
Cs	T	$C_1(2)$	3	3
$2SO_4$	T	$C_1(2)$	6	6
$2SO_4$	R	$C_1(2)$	6	6
$2SO_4$	I	$C_1(2)$	18	18
	Total		$\Gamma = 42\ A' + 42\ A''$	
	Acoustic		$\Gamma_{ac} = 2\ A' + A''$	
	Vibrational		$\Gamma_{vib} = 40\ A' + 41\ A''$	

The best scattering geometry for verifying the predictions of the site group analysis is $y(xz)\overline{y}$, since it does not show a mixture of longitudinal and transverse modes in the Raman spectra. From figure 2(d) we observe clearly all six ν_3 modes distributed into two well separated regions ($\widetilde{\nu} < 1150$ and $\widetilde{\nu} > 1150\,\mathrm{cm}^{-1}$). Figure 3 shows the polarized Raman spectra recorded in the wavenumber region $300 < \widetilde{\nu} < 700\ \mathrm{cm}^{-1}$. According to Oh *et al* [22], besides ν_2 and ν_4 SO_4 modes, Li translational modes must also be observed in this spectral region. We have assumed, on the basis of the results shown in figure 4 and discussed below, that Li, Cs and Rb ions occupy $C_1(2)$ local site symmetries. Hence, six T_{Li}, four ν_2 and six ν_4 modes are expected to be observed. Since broad and asymmetric bands are observed, we use a computer-based program to determine how many Raman modes are indeed present in the band. Deconvolution of overlapping bands was performed by using a non-linear least-squares fit assuming Lorentzian line profiles. In this, we observe from figure 3(d) a Li translational mode oscillating at 400 cm^{-1}, four ν_2 modes in the range $425 < \widetilde{\nu} < 550\ \mathrm{cm}^{-1}$ and four ν_4 modes in the range $600 < \widetilde{\nu} < 675\ \mathrm{cm}^{-1}$. Four other modes were observed in the range $300 < \widetilde{\nu} < 425\ \mathrm{cm}^{-1}$. Similar results are also obtained from figures 3(a)–3(c).

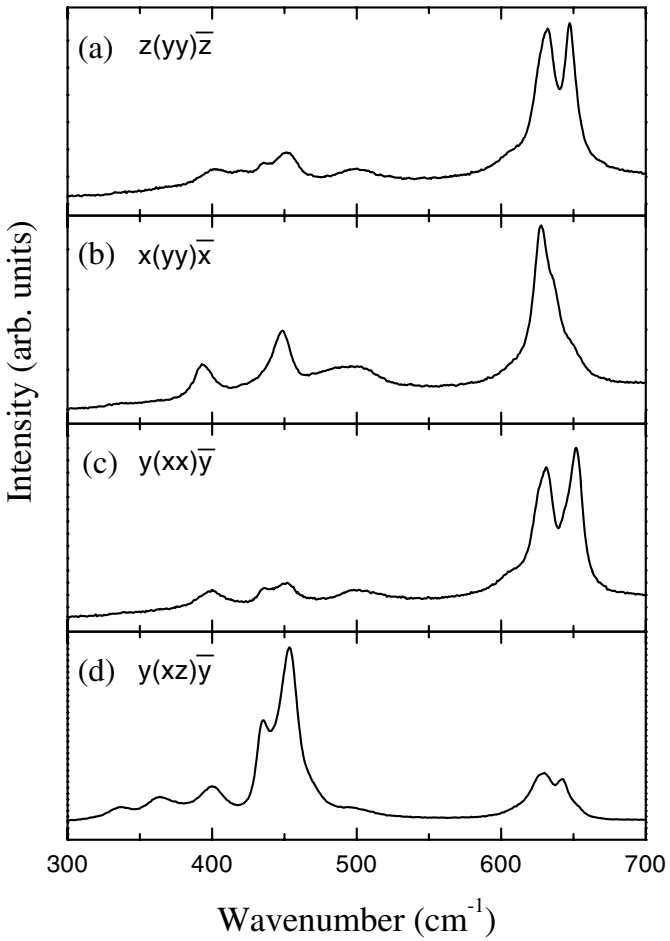

Figure 3. Polarized Raman spectra of LRCS in the wavenumber range of ν_2 and ν_4 internal modes of the SO_4 ion.

Finally, let us discuss the low-wavenumber region of LRCS crystal, where the external modes of SO_4, Li, Cs and Rb ions are expected to be observed. Without performing a lattice dynamics calculation, it is very difficult to correctly assign the vibrations observed. However, by comparing the LRCS Raman spectrum for different values of x, we were able to identify some. In figures 4(a) and 4(c) we show the Raman spectrum recorded in the $y(xx)\overline{y}$ scattering geometry for $x = 1.0$, 0.75 and for $x = 0.4$, 0.0, respectively. Notice that the wavenumber of the vibration at 143 cm^{-1} for $x = 0.0$ (LCS) increases with increasing Rb content ($\widetilde{\nu} = 188$ cm^{-1} for $x = 1.0$ (LRS)). This result allow us to associate this band with a heavy-ion translation. However, for $x = 0.5$ we observe from figure 4(b), besides the appearance of two modes oscillating at 120 and 225 cm^{-1}, two vibrations at $\widetilde{\nu} = 160$ and 180 cm^{-1}, which we associate with Cs and Rb translational modes, respectively. This latter result indicates that in the LRCS crystal structure, neither Rb nor Cs atoms are randomly distributed; rather, they now occupy non-equivalent $C_1(2)$ site symmetries.

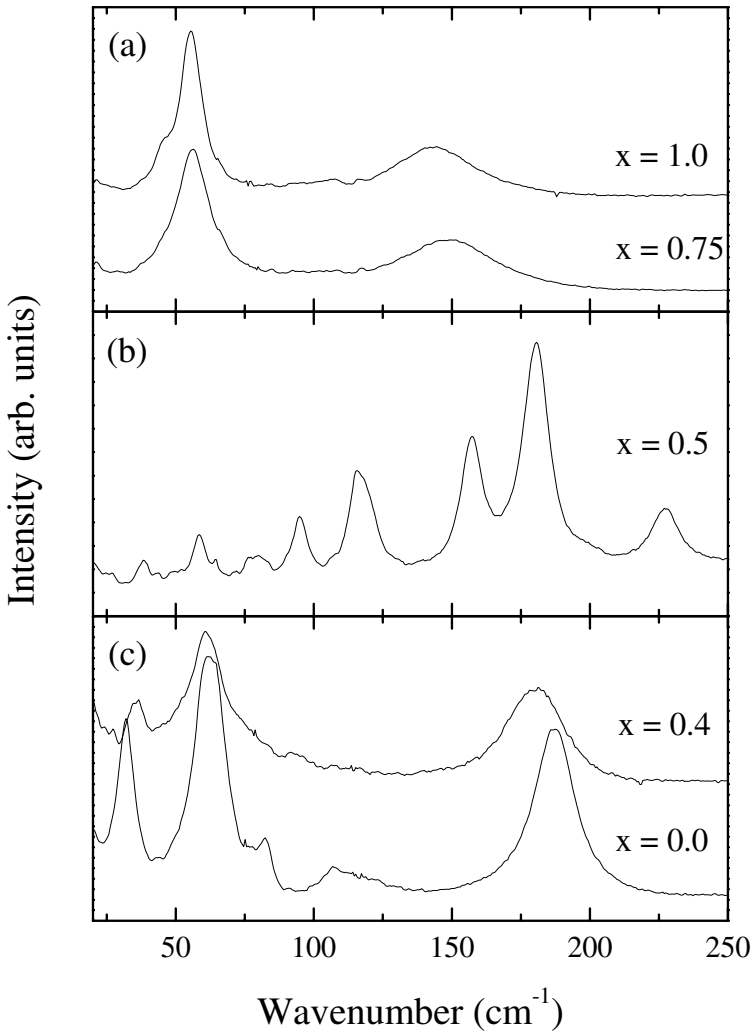

Figure 4. The low-frequency Raman spectrum of $LiRb_{1-x}Cs_xSO_4$ crystals in the $y(xx)\bar{y}$ orientation taken at 300 K. (a) $x = 1.0$ and 0.75; (b) $x = 0.5$; and (c) $x = 0.4$ and 0.0.

Katkanant's [13] calculation also needs to be commented on because it shows that the lattice energy increases uniformly with the Cs concentration. That result suggests a continuous transformation between the LCS and LRS structures, without any new phase. However, Katkanant in the simulations supposed a random distribution of Rb and Cs ions. Thus, our proposal of an ordered structure does not contradict those simulations.

4. Conclusions

In conclusion, we have reported on the growth and structural analysis of the $x = 0.5$ member of the $LiRb_{1-x}Cs_xSO_4$ system. The LRCS crystal was grown at a constant temperature of 40 °C and pH = 9.0 from aqueous solution containing a stoichiometrically proportioned mixture of Li_2SO_4, $CsSO_4$ and Rb_2SO_4. From the x-ray diffraction and polarized Raman data, we determined that LRCS crystals at 300 K have a monoclinic lattice belonging to factor group C_s. The unit cell contains four formula units, where the four SO_4 ions are in two non-equivalent $C_1(2)$ local site symmetries, the two Rb and two Cs ions each occupy a $C_1(2)$ local site symmetry, while the four Li ions are in two $C_1(2)$ local site symmetries. Of the 40 A′ and 41 A″ optical vibrations expected, 28 A′(TO + LO) and 29 A″(LO) are observed. The reason that fewer modes than formally predicted are observed in both A′ and A″ scattering geometries is twofold:

(i) some modes have very weak polarizability derivatives leading to very weak bonds which are not seen; and
(ii) the correlation field splittings may be so small that the factor group components are not completely resolved.

Further study of the temperature- and hydrostatic-pressure-dependent behaviour of LRCS Raman phonons is in progress and will be the subject of a future publication.

Acknowledgments

The authors would like to thank FUNCAP, CNPq and FINEP for financial support.

References

[1] Aleksandrov K S 1993 *Kristallografiya* **38** 128
[2] Unruh H G 1981 *Ferroelectrics* **36** 359
[3] Melo F E A, Lemos V, Cerdeira F and Mendes Filho J 1987 *Phys. Rev.* B **35** 3633
[4] Silveira E S, Freire P T C, Pilla O and Lemos V 1995 *Phys. Rev.* B **51** 593
[5] Freire P T C, Pilla O, Lemos V, Melo F E A, Guedes I and Mendes Filho J 1995 *Rev. High Pressure Sci. Technol.* **7** 137
[6] Mashiyama H, Hasebe K, Tanisaki S, Shiroishi Y and Sawada S 1979 *J. Phys. Soc. Japan* **47** 1198
[7] Mestres L, Martinez-Sarrion M L, Baccali A, Simkin V G, Smirnov L S and Balagurov A M 1999 *Crystallogr. Rep.* **44** 78
[8] Kunishige A and Mashiyama H 1987 *J. Phys. Soc. Japan* **56** 3189
[9] Pietrazko A 1981 *Acta Crystallogr.* A **37** C109
[10] Hasebe K and Asahi T 1989 *Ferroelectrics* **96** 63
[11] Mel'nikova S V, Grankina V A and Voronov V N 1994 *Phys. Solid State* **36** 612
[12] Mel'nikova S V, Vasil'ev A D, Voronov V N and Bovina A F 1995 *Phys. Solid State* **37** 1387
[13] Katkanant V 1995 *Phys. Rev.* B **51** 146
[14] Damem T C, Porto S P S and Tell S B 1966 *Phys. Rev.* **142** 570
[15] Rodriguez-Carvajal J, Fernandez-Diaz M T and Martinez J L 1991 *J. Phys.: Condens. Matter* **3** 3215
[16] Louer D and Louer M 1972 *J. Appl. Crystallogr.* **5** 271
[17] Boultif A I and Louer D 1991 *J. Appl. Crystallogr.* **24** 987

[18] De Wolff and Visser J 1969 *J. Appl. Crystallogr.* **2** 89
[19] Azároff L V 1968 *Elements of X-ray Crystallography* (New York: McGraw-Hill)
[20] Fateley W G, McDevitt F R N T and Bentley F F 1972 *Infrared and Raman Selection Rules for Molecular and Lattice Vibrations: the Correlation Method* (New York: Wiley)
[21] Rousseau D L, Bauman R P and Porto S P S 1981 *J. Raman Spectrosc.* **10** 253
[22] Oh K H, Cho J H and Kim S-B 1993 *Appl. Spectrosc.* **47** 999